Measurement of the density shift of the H_2 $Q(0-5)$ transitions from 295 to 1000 K

Larry A. Rahn
Combustion Research Facility, Sandia National Laboratories, Livermore, California 94551-0969

G. J. Rosasco
Center for Chemical Technology, U.S. National Institute of Standards and Technology, Gaithersburg, Maryland 20899
(Received 17 October 1989)

We report results of a high-resolution inverse Raman spectroscopy study of the dependence on temperature and rotational quantum number J of the Raman Q-branch self-density-shift coefficients of pure (natural) hydrogen. The population-correlated J dependence of these coefficients, previously established at lower temperatures as a "coupling shift," is observed to persist, almost independent of temperature, up to 1000 K. The temperature dependence of the overall shift is found to disagree above 500 K with extrapolations of recent theoretical calculations.

INTRODUCTION

The characteristics of the vibration-rotation spectrum of H_2 are of interest for many practical applications as well as for basic studies of molecular spectra and collisional interactions. Diagnostic measurements using Raman spectroscopy, for example, in combustion[1] and plasma[2] environments, require accurate spectral models for interpretation. The hydrogen molecule is also amenable to detailed quantum calculations and has often been a "meeting ground" for theoretical and experimental results. For example, transition frequencies and Raman line strengths of the isolated molecule can now be calculated quite accurately.[3] Recent progress has also been made in the calculation[4,5] of the effects of collisions on the vibrational spectrum. Experimental measurement of collisional density-shift and broadening coefficients and their temperature dependences are of particular interest since they provide information on both the angular and radial dependence of the molecular interaction potential.[5]

Numerous studies of the H_2 Raman Q-branch transitions have been performed since Rasetti[6] first reported the H_2 Raman spectrum 60 years ago. The early mercury-lamp-excited work provided molecular constants,[7] as well as density-shift and broadening coefficients at high densities.[8-10] These measurements, as well as reports[11-15] of line-shift measurements in pure H_2 since then, have been limited to temperatures at or below 315 K with the exception of results[12,14] on $Q(1)$ to near 500 K. Accurate line positions obtained from Raman measurements in flames and from electric-quadrupole-absorption and field-induced-absorption spectra have been summarized by Jennings *et al.*[16] Density-shift and broadening data from the absorption spectroscopies have been compared recently to Raman data and theory by Kelley and Bragg.[5]

In this paper we report measurements of the linear density-shift coefficients for the $J=0-5$ Q-branch transitions in pure H_2 from 295 to 1000 K using high-resolution inverse Raman spectroscopy IRS. This range of J and T significantly extends previous experimental studies. Our room-temperature data are analyzed in conjunction with previously reported high-density measurements[9,15] and we report new values for the linear, quadratic, and cubic density-shift coefficients. The zero-density Q-branch frequency positions derived from this analysis are compared with previous measurements[16] and *ab initio* calculations.[3] Higher-temperature measurements are compared to previous high-resolution measurements[12,14] and theoretical predictions[5] up to 500 K. Of particular interest in the analysis of the high-temperature shift data is the examination of the observed J and T dependence in light of the coupling shift previously established by May, Welsh, and co-workers[9,10] and also confirmed by Lallemand and Simova,[12] and Bischel and Dyer.[14] Although our higher-temperature data reveal a more complicated J dependence than can be explained by the coupling shift alone, we are able to identify a coupling-shift contribution up to 1000 K. This contribution is observed as a negative shift with increasing J-state population and is almost temperature independent throughout the high-temperature range. This trend is almost identical to that observed previously in the range 85-315 K.[9,10] The fact that the magnitude, sign, and T dependence of the coupling shift cannot be explained by current theory[5] provides strong evidence for the need to improve our knowledge of the vibrational-state dependence (particularly for the repulsive core portion) of the H_2-H_2 intermolecular potential.

EXPERIMENT

The IRS spectrometer used in this study has a resolution of ~ 0.0015 cm^{-1} and uses a pulse-amplified [$\sim$22-ns full width at half maximum (FWHM)] cw dye laser as a pump and a single-frequency argon-ion laser as a probe. The probe-laser frequency is locked to a temperature-stabilized etalon, which also provides pump-laser-transmission fringes that are used to linearize the pump-

laser scan (see below). The Q-branch transition frequencies are determined from measurements of the frequency differences of the pump (i.e., the cw dye laser) and the probe lasers. A traveling corner-cube wave meter and the temperature-stabilized etalon (750-MHz free spectral range) are used to provide a precision of ± 0.001 cm^{-1} (30 MHz) in the measurement of the frequency differences between Q-branch transitions for ranges of frequency difference up to tens of cm^{-1}. The absolute accuracy of this measurement is found (see below) to be systematically shifted ~ 0.003 cm^{-1} from more accurate electric-quadrupole-absorption measurements.[16] A relative accuracy of ± 0.0005 cm^{-1} is achieved for the frequency scan over an individual line, since this measurement generally depends only on the interpolating interferometer. The signal voltages in IRS are linear in the powers of the pump and probe lasers. The intensity axis of the spectrum is determined after a pulse-by-pulse normalization for laser powers and the averaging of the normalized signal for typically 40 Raman-pump-laser pulses.

The measurements were made in an internally heated pressure vessel at pressures up to 50 atm. The vessel is water cooled and equipped with fused silica windows. The furnace contained within the vessel consists of an insulated ceramic tube with a heater element applied to its outer surface. The thermal gradient along the optical axis of the tube is maintained by two silica cylinders that confine a central heated gas to a volume approximately 4 cm long. The gas volume is further restricted to a diameter of 6 mm by a molybdenum tube spacer. The silica cylinders have polished spherical surfaces with radii that are concentric with the center of the heated region. The Raman-pump- and probe-laser beams are crossed inside the heated gas volume at a small angle (0.018 rad) at the focus of a 470-mm focal-length lens. The focused-beam diameters are approximately 100 μm. We measured the gas pressure in the vessel with transducers accurate to ± 0.2 atm at 50 atm, or with capacitance manometers accurate to ± 0.01 atm below 10 atm, and calculated amagat density units using expressions for virial coefficients including quantum deviations given in Ref. 17. A $\sim 3\%$ maximum deviation below ideal-gas density was found at 295 K and 50 atm. The temperature was monitored with two thermocouples outside the surface of, but not in physical contact with, the heated ceramic tube. One was located near the heater and the other near a small hole centered on the molybdenum tube. In separate experiments on N_2, we have observed differences between the two thermocouple readings as large as 10 K at 600 K that were ~ 60 K lower than the temperature of the gas obtained from fits to N_2 Q-branch spectra. These differences were independent of pressure and were smaller at higher temperatures. In the experiments reported here, the difference between the thermocouple readings was reduced, presumably due to the $\sim 7x$ increase in thermal conductivity of H_2 over that of N_2. The maximum observed difference in H_2 was ~ 6 K at 725 K, and it was only ~ 2 K at 450 and 1000 K. From these observations, we estimate the probable systematic errors in our temperature measurement to be $+40$ K at 725 K and $+15$ K at 450 and 1000 K.

ZERO-DENSITY LINE POSITIONS

With a few exceptions (discussed below), the density-shift coefficient was determined by comparing the measured line position at high density (determined by the 50-atm pressure limit of the furnace) to the zero-density line position. The zero-density frequencies were determined by wave-meter measurements and line-profile fits to spectral scans at low (0.05–1 atm) pressure. The accuracy of the measurements of the $Q(0)$ and $Q(2-5)$ lines relative to the $Q(1)$ line was improved using the known spacing of the 750-MHz interferometer fringes that were simultaneously acquired with the Raman data. Finally, the line positions were corrected for Stark shifts[18] due to the pump-laser power and for density shifts. The (small) density corrections necessary to determine the zero-density frequencies from the 0.05–1 atm measurements were determined from approximate density-shift coefficients derived from the literature and/or from preliminary analysis of our 50-atm data. The Stark-shift correction was determined from the pump power dependence of the $Q(1)$ transition frequency measured at 0.049 amagat and room temperature, shown in Fig. 1. The slope of the straight-line fit [$-1.4(5)\times 10^{-5}$ cm^{-1}/kW (the estimated error is shown in parentheses)] is consistent with the expected shift[19] for an effective pump-beam diameter of 70 μm. While the Stark correction is only approximate, it is also very small for the laser powers used (5–140 kW, peak). The total uncertainty arising from the Stark and density-shift corrections was less than 0.001 cm^{-1} for all of the zero-density line-position determinations.

We can also determine a value for the zero-density frequency of the $Q(1)$ transition from the experimental data displayed in Fig. 2. This set of measurements as a function of density at 1000 K follows the displayed straight-line fit with a rms deviation of 5×10^{-4} cm^{-1}. As a measure of the consistency of our data, we note that when the frequency intercept in Fig. 2 is corrected for the 5-kW pump power and that of Fig. 1 is corrected for the density shift,[14] they are separated by only 4×10^{-4} cm^{-1} with

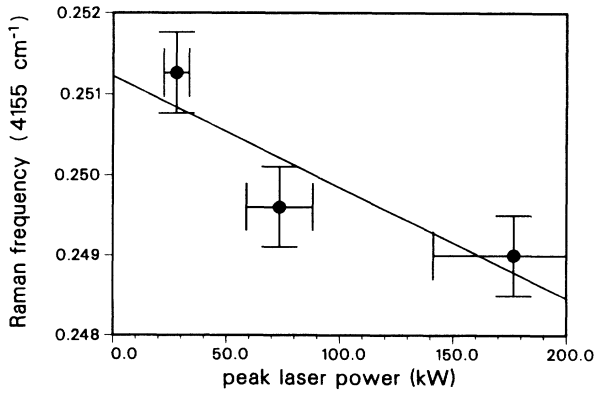

FIG. 1. The frequency of the $Q(1)$ transition of H_2 at 295 K is plotted vs peak laser power (symbols). The zero-power intercept is at 4155.2512(3) cm^{-1} and the slope is $-1.4(5)\times 10^{-5}$ cm^{-1}/kW.

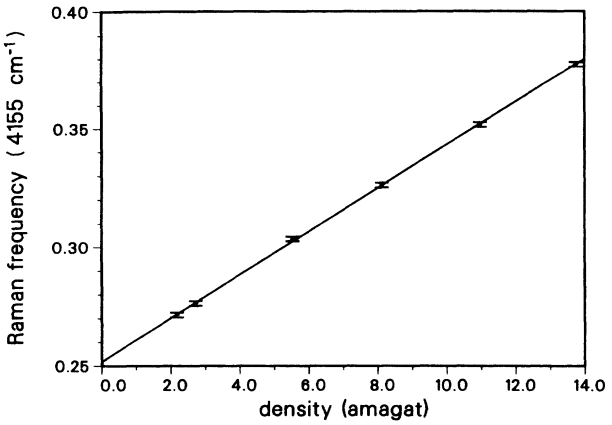

FIG. 2. The frequency of the $Q(1)$ transition of H_2 at 1000 K is plotted vs density (symbols). The slope (density-shift coefficient) of the straight-line fit is 0.009 16(11) cm^{-1}/amagat, and the zero-density intercept is at 4155.2517(2) cm^{-1}.

an average of 4155.2516(5) cm^{-1}. We have taken the -0.0031-cm^{-1} offset between this value and that reported by Jennings *et al.*[16] as a systematic error in our wave meter (we have observed a -0.0023-cm^{-1} offset in measurements[20] on CO). In Table I, the $Q(0)$ and $Q(2-5)$ measurements, corrected for density, laser power, and systematic wave-meter error, are compared to measurements reported in Ref. 16 and the theory in Ref. 3. The agreement with previous results is excellent, with improvements in the accuracy of the $Q(4)$ and $Q(5)$ transitions. The agreement with the theory is also very good, even though a systematic offset of ~ 0.02 cm^{-1} below the experimental values is apparent.

DENSITY-SHIFT COEFFICIENTS

As noted above, we performed a detailed density study only for the $Q(1)$ line at 1000 K. While a linear density dependence was adequate for our analysis of these data, previous workers have found it necessary to consider also a quadratic dependence for higher-density measurements. Recently Moulton *et al.*[15] reported linear and quadratic density-shift coefficients for H_2 at room temperature for densities up to 1400 amagat. These coefficients are considerably larger (see Table II) than those obtained by May *et al.*[9] from measurements up to 400 amagat. The quadratic density dependence reported by these authors would contribute 10%–20% of the shift that we measured at 45 amagat and 295 K, thus contributing a significant uncertainty to the linear density-shift coefficients.

To account for the nonlinear dependence of shift on the density at 295 K, we analyzed our data along with results from Refs. 9 and 15 according to the relation

$$\omega_J = \omega_J^0 + \alpha_J \rho + \beta_J \rho^2 + \gamma_J \rho^3 \ . \tag{1}$$

In Eq. (1), ρ is the density in amagat units, ω_J and ω_J^0 are the frequency (cm^{-1}) of the $Q(J)$ transition at density of ρ and 0, respectively. Because the shift data of Ref. 15 were not reported in tabular form, we generated representative data by calculating a value for ω_J at nine densities between 340 and 1400 amagat using the reported coefficients (Table II). We analyzed all of the available data by fitting the coefficients α, β, and γ using a weighted least-squares fit for each value of J at 295 K. A systematic offset ($\Delta\omega_s$), added to the data from Refs. 9 and 15, was also allowed to vary.

We found that all of the data could be fit, consistent with the experimental errors, by Eq. (1), except that $\Delta\omega_s$ for $J=0$ and 1 of Ref. 15 was larger than the quoted 0.2-cm^{-1} error. The highest-density data (Ref. 15) are well described by the cubic density term in Eq. (1) with linear and quadratic coefficients close to those reported in Ref. 9. The values of the parameters resulting from these fits are shown in Table III. The values in parentheses are the estimated errors in units of the least significant digit. The first error shown in parentheses for α is the value that must be added to α to maintain agreement with our shift measurements when β and γ are set to zero. The second value in parentheses is the estimated error due solely to experimental error. This estimate includes the effects of wave-meter accuracy and variations due to ± 1 K errors in the temperature measurement. The errors shown for β and γ are the variations which increase the rms variation of the data of Ref. 15 from the fit to ~ 0.4 cm^{-1} when the $\Delta\omega_s$ are allowed to float. The estimated errors shown for $\Delta\omega_s$ are just the rms variation of the best fit to the associated data. An example of the fit obtained is shown in Fig. 3 for the $Q(2)$ transition. Clearly, neither of the quadra-

TABLE I. Transition frequencies (cm^{-1}) for the $Q(J)$ lines of H_2 at zero density. Δ columns are given by Δ_1 equals experimental minus previous values and Δ_2 equals experimental minus theoretical values. The estimated errors are shown in parentheses.

J	Experiment[a]	Previous[b]	Δ_1	Theory[c]	Δ_2
0	4161.1673(14)	4161.1687(4)	−0.0014	4161.147(15)	0.020
1	4155.2547(5)	4155.2547(1)	0	4155.235(15)	0.020
2	4143.4651(14)	4143.4660(3)	−0.0009	4143.446(15)	0.019
3	4125.8728(14)	4125.8739(4)	−0.0011	4125.855(15)	0.018
4	4102.5822(12)	4102.5820(40)	0.0002	4102.566(15)	0.016
5	4073.7326(14)	4073.743(30)	−0.0104	4073.717(15)	0.016

[a]Adjusted so that $Q(1)$ agrees with that of Ref. 16.
[b]Reference 16.
[c]Reference 3.

TABLE II. Coefficients from Refs. 9 and 15 describing the room-temperature H_2 density shift [using the notation of Eq. (1) with $\gamma=0$]. The estimated errors are shown in parentheses.

	Reference 9			Reference 15		
J	ω_J^0 (cm^{-1})	α (10^{-3} cm^{-1}/amagat)	β (10^{-6} cm^{-1}/amagat^2)	ω_J^0 (cm^{-1})	α (10^{-3} cm^{-1}/amagat)	β (10^{-6} cm^{-1}/amagat^2)
0	4161.151(14)	−2.35(17)	5.60(40)	4162.1(2)	−5.76	10.6
1	4155.212(12)	−3.14(15)	4.86(35)	4156.3(2)	−7.27	10.7
2	4143.466(13)	−2.07(16)	5.77(37)	4144.7(2)	−8.50	14.1
3	4125.861(14)	−2.25(17)	6.79(40)	4127.3(2)	−8.94	14.6
4				4103.8(2)	−7.40	13.8
5				4074.3(2)	−5.10	11.9

tic expressions for ω_J quoted in Refs. 9 or 15 is able to describe all of the data. The inclusion of the cubic term thus allows a consistent description of the high-density data and allows reliable linear density-shift coefficients to be extracted from our room-temperature measurements at ~45 amagat. We note, with respect to the latter, that variations in α required by the errors assigned to β and γ in Table III are less than the experimental errors assigned to α.

Linear density-shift coefficients were also determined from the measurements at elevated temperature and are listed in Table IV. These values are determined assuming that β and γ were equal to zero, since higher-density measurements have not been performed at elevated temperatures. May *et al.*[9] did report, however, values for β at 85 K for $J=0$ and 1 that were not significantly different from the 300-K values. The change in our determination of α that would result from temperature-independent values of β and γ is indicated by the first number in the parentheses following each entry in Table IV. This number, and the one following it indicating the random error estimate, are in units of the least significant digit of the preceding entry.

The error estimates shown in Table IV do not include the effects of the systematic errors in the measurement of the sample-gas temperature discussed earlier. These errors in T imply systematic errors in the density and therefore in the magnitudes of the density-shift coefficients. The strong temperature dependence of these coefficients also leads to an error related to systematic errors in T. These two errors tend to cancel at high temperatures, resulting in a -0.05×10^{-3} cm^{-1}/amagat (averaged over J) correction at 1000 K when the actual gas temperature is assumed to have been 1015 K. A similar correction of -0.2×10^{-3} cm^{-1}/amagat results from systematic errors in T at both 450 and 725 K for temperature variations of +15 and +40 K, respectively. The largest systematic error (-0.24×10^{-3} cm^{-1}/amagat) is calculated for $J=1$ at 450 K and is due to the strong temperature sensitivity of this coefficient.

COMPARISON WITH OTHER RESULTS AND THEORY

The previously reported values of the room-temperature density shift in pure H_2 are compared with our measurements in Table V. The agreement is generally good, except for the early values reported by May *et al.*[8] and those reported by Moulton *et al.*[15] The differences between the values of Refs. 8 and 9 have been reconciled in the latter paper, and we have demonstrated that those of Ref. 15 should be reinterpreted. The remaining variations are largely accounted for by the strong temperature dependence of the coefficients ($\sim0.026\times10^{-3}$ cm^{-1}/amagat/K for $J=1$). The agreement with the measurements of Bischel and Dyer[14] at 298 K is, in fact, excellent if one also accounts for the nonlinearity of the shift with density and non-ideal-gas effects at their highest (12 amagat) densities.

The only previous reports of H_2 density-shift measurements at elevated temperature were studies on $Q(1)$ up to 488 K (Ref. 12) and 474 K.[14] For comparison with our results (see Table IV), the value reported at 454 K by Lallemand and Simova[12] is used, and the temperature depen-

TABLE III. Coefficients from Eq. (1) derived by fitting 295-K Q-line shifts for $J=0$, 2–5 at ~45 amagat and room-temperature data from Refs. 9 and 15. The estimated errors are shown in parentheses (see text).

J	α (10^{-3} cm^{-1}/amagat)	β (10^{-6} cm^{-1}/amagat^2)	γ (10^{-9} cm^{-1}/amagat^3)	$\Delta\omega_s$ (Ref. 9) (cm^{-1})	$\Delta\omega_s$ (Ref. 15) (cm^{-1})
0	−2.28(+18,±6)	4.1(8)	3.5(14)	0.012(26)	−0.447(057)
1	−3.38(+18,±5)	4.1(7)	3.1(4)	0.012(28)	−0.478(141)
2	−2.05(+19,±6)	4.1(7)	4.4(5)	−0.011(27)	−0.199(161)
3	−2.07(+25,±6)	4.8(7)	4.1(6)	0.012(27)	−0.104(120)
4	−1.81(+29,±5)	6.2(7)	3.1(5)		−0.037(080)
5	−1.70(+28,±6)	6.1(7)	2.7(5)		−0.099(113)

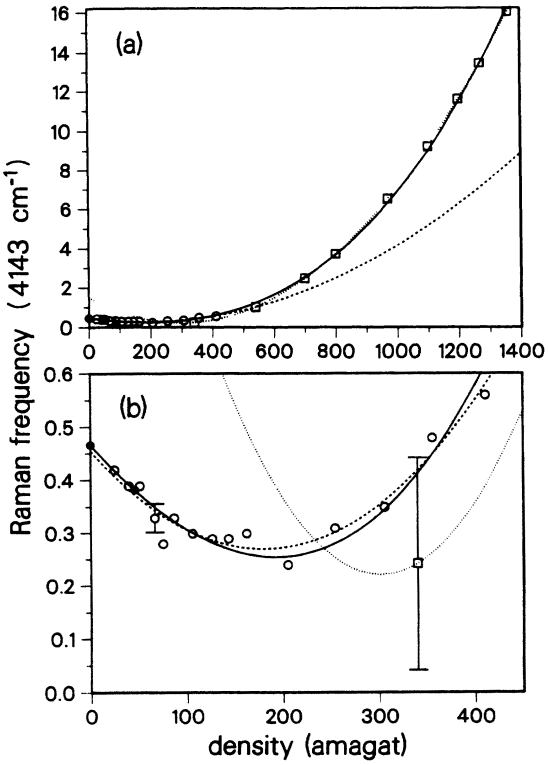

FIG. 3. The frequency of the $Q(2)$ transition of H_2 at 295 K is plotted vs density (symbols: ○: Ref. 9; □: Ref. 15; ●: this work) up to 1400 amagat (a) and up to 450 amagat (b). The dashed and dotted lines are the reported quadratic fits to the data in Refs. 9 and 15, respectively (see Table II). The solid line is a cubic fit to all of the data (see Table III).

dence reported by Bischel and Dyer[14] is used to calculate a value for 450 K. The latter coefficient disagrees with ours and that of Ref. 12, but a quadratic coefficient, $\beta=17(2)\times10^{-6}$ cm^{-1}/amagat^2, was also reported for the 474-K measurement. This value of β is high compared to that in Table III and was not observed by Lallemand and Simova at even higher densities. The origin of this observed quadratic density dependence is uncertain, but including it in a calculation to predict the shift at 8 amagat produces a result that is somewhat closer to our measurement. We also note that our measurement is subject to a possible systematic error (discussed above) of -0.24×10^{-3} cm^{-1}/amagat.

In Figs. 4 and 5, we present different approaches to a possible systemization of the trends in the J and T dependence of the self-density-shift coefficients. Previous studies[5,8–10,12] of the J dependence have been made at room temperature and below, and have found that the shifts decrease linearly with increasing J-state population and are well described by the relation

$$\alpha_J=\alpha_i+\alpha_c(n_J/n)\ . \tag{2}$$

In Eq. (2), α_i and α_c are (possibly temperature-dependent) constants and n_J/n is the fractional population of the rotational state J. This dependence is predicted by the coupling-shift theory (discussed below) originally proposed for the gas phase by May *et al.*[9] In Fig. 4 we examine this approach explicitly by plotting α_J versus n_J/n. The lower-temperature measurements reported in Ref. 10 (open symbols) have also been plotted for comparison to those reported here (solid symbols). It is clear that the J dependence at high temperatures does not adhere to the strictly linear dependence on population that appears to hold for the lower-temperature data. In fact, inspection of Table IV reveals a trend at high temperatures toward J ordering, rather than population ordering of the α_J. We have attempted to separate these trends by fitting a straight line to a small range of J with the largest variation in population [$Q(1-3)$] for the α_J above room temperature. These fits are shown as lines in Fig. 4 along with similar fits to the lower-temperature data that include all of the J states. The slopes of the straight-line fits are nearly independent of temperature, indicating a coupling shift (α_c) with a value[9,10,12,14] of -1.7 to -2.2×10^{-3} cm^{-1}amagat^{-1} between 85 and 1000 K.

We see in Fig. 4 that, while the J dependence at high temperatures does exhibit a correlation with population, there are variations that are not predicted by a simple coupling-shift model. In Fig. 5 the J dependence of the shift coefficients at each temperature is shown relative to the shift of the $Q(0)$ line before, 5(a), and after, 5(b), the removal of the population trend expressed by fits to Eq. (2). We note that, in Fig. 5(a), the overall trend with J varies significantly with increasing temperature. The

TABLE IV. Linear density-shift coefficients derived from Q-branch line shifts for $J=0-5$ measured at temperatures from 450 to 1000 K. The estimated errors are shown in parentheses (see text). The coefficients are in units of 10^{-3} cm^{-1}/amagat.

J	450 K	454 K[a]	450 K[b]	725 K	1000 K
0	1.22(−13,±8)			5.28(−8,±13)	8.45(−6,±18)
1	0.70(−12,±5)	0.8(2)	0.05(3)	5.53(−7,±8)	9.16(−5,±11)
2	1.55(−13,±8)			6.04(−8,±13)	9.73(−6,±18)
3	1.48(−19,±8)			5.94(−12,±13)	9.65(−9,±18)
4	1.99(−19,±8)			6.56(−12,±13)	10.34(−9,±18)
5	2.11(−19,±8)			6.70(−12,±13)	10.46(−8,±18)

[a]Reference 12.
[b]Reference 14.

TABLE V. A comparison of linear density-shift coefficients reported for H_2 Q-branch transitions at 295–315 K. The coefficients are in units of 10^{-3} cm^{-1}/amagat. The estimated errors are shown in parentheses. RT refers to measurements reported at room temperature.

J	This work (295 K)	Ref. 14 (298 K)	Ref. 9 (300 K)	Ref. 10 (315 K)	Ref. 13 (298 K)	Ref. 8 (RT)	Ref. 15 (RT)	Ref. 11 (RT)	Ref. 12 (297 K)
0	−2.28(6)	−2.14(17)	−2.35(17)	−2.29(13)	−2.15(30)	−3.70	−5.76		
1	−3.38(5)	−3.20(3)	−3.14(15)	−3.05(14)	−3.00(30)	−4.45	−7.27	−3.2	−3.0(1)
2	−2.05(6)		−2.07(16)	−2.22(21)	−1.35(30)	−3.40	−8.50		
3	−2.07(6)		−2.25(17)	−1.96(26)	−1.35	−3.30	−8.94		
4	−1.81(6)						−7.40		
5	−1.70(6)						−5.10		

variations for $J=1$ and 3 are strongly temperature dependent, decreasing in magnitude at $J=1$ and increasing for $J=3$ with increasing temperature. After removing the coupling shift, we find the relatively simple J dependence illustrated in Fig. 5(b). This remaining J dependence of the shift coefficients shows a positive shift that increases rapidly between $J=0$ and 1, and more uniformly at higher J with a relatively uniform temperature dependence. The simplification of the J dependence in Fig. 5(b) appears to support the separation of the trends toward J ordering at high temperature and population ordering at low temperature. Further analysis of the J-ordered trend could be easily performed using the energy-corrected-sudden-scaling theory reported by DePristo.[21] We have not pursued such an analysis, however, since the results provide information that is not transferable to other experiments without more detailed scattering calculations.

The overall temperature dependence of the measured H_2 shift coefficients is compared to an extrapolation of the theoretical prediction of Kelly and Bragg[5] in Fig. 6.

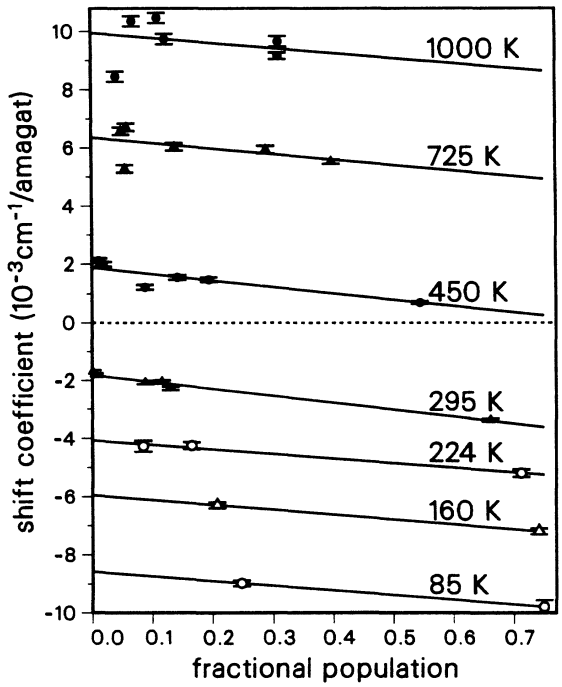

FIG. 4. Linear density-shift coefficients from the present work (first, fourth, and fifth columns of Table IV and the first column of Table V, solid symbols) and from Ref. 10 (open symbols) at lower temperatures are plotted vs the fractional population in the associated rotational state. The solid lines are straight-line fits to the data at each temperature. At 450 K and above, only the $Q(1)$, $Q(2)$, and $Q(3)$ values were used in the fits.

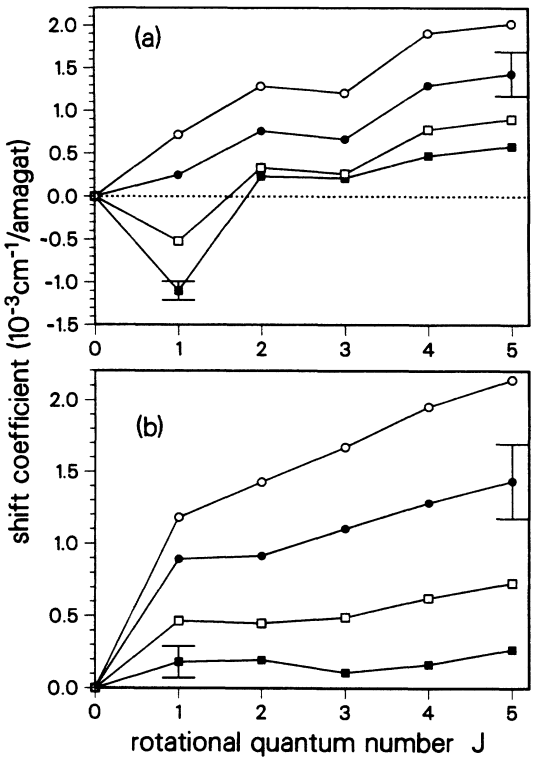

FIG. 5. Linear density-shift coefficients from the present work (first, fourth, and fifth columns of Table IV and the first column of Table V) relative to the value for $Q(0)$ at each temperature are plotted vs J in (a). The symbols indicate temperature; ○: 1000 K; ●: 725 K; □: 450 K, and ■: 295 K. In (b) the deviation of the linear density-shift coefficients from the straight-line fits in Fig. 4, with the deviation for $Q(0)$ at each temperature subtracted, is plotted vs the rotational quantum number (J).

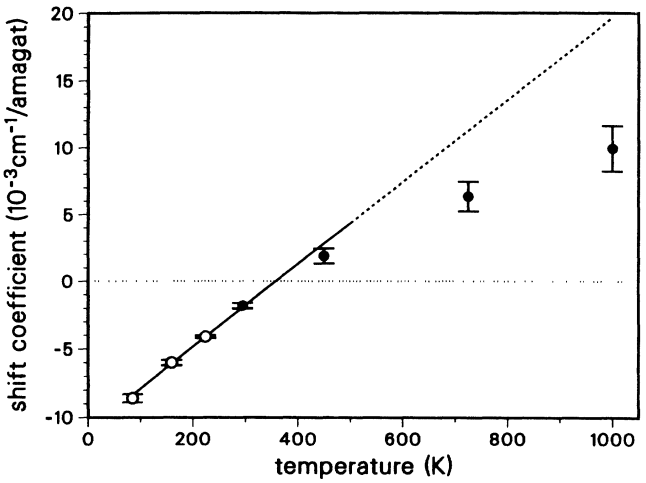

FIG. 6. The overall temperature dependence of the linear density-shift coefficients is indicated by plotting the zero-population intercepts of Fig. 4 (solid symbols are data from this work, and open symbols are from Ref. 10) vs temperature. The solid (dashed) line is a fit (extrapolated fit) to the theoretical shifts from Ref. 5.

These authors varied the interaction potential used in their calculation to fit, among other data, the (85–315 K) Raman shift data reported by Looi *et al.*[10] with the coupling shift removed. The calculation displays a linear dependence on temperature from 85 up to 500 K and a linear fit to it is compared to our data and the lower-temperature data[10] in Fig. 6 (solid line). The experimental points are the intercepts at zero population (α_i) taken from Fig. 4. The (dashed line) extrapolation of the fit to the theoretical calculations to 1000 K also is shown in the figure. Clearly, the experimental shift coefficients above room temperature are much less positive than those predicted by a simple extrapolation of the calculation.

THE COUPLING SHIFT

The coupling-shift theory, mentioned previously in reference to Eq. (2), was proposed by May *et al.*[9] to explain the observed[8,9] correlations between the α_J and the relative population of the Jth rotational state. The theory predicts a collisional phase shift arising from the in-phase coupled oscillation of pairs of identical, colliding molecules. While symmetric and antisymmetric combinations of the molecular wave functions produce opposite shifts, the Raman selection rules allow only the symmetric combination to contribute, and the resulting phase shifts accumulate, producing a density shift with a J dependence that is proportional to the fractional population of the associated rotational level. This theory has been discussed often in the literature,[5,8–10,12,14] and the effect is also observed when the ortho- to parahydrogen ratio is modified.[12,14] This coupled-mode analysis is based on ideas initially developed to explain frequency shifts that depended on the ortho-para composition in solid hydrogen.[22]

For the gas phase, the coupling shift is probably better described as a resonance-collision shift. Since the early work of May *et al.*, the resonance-collision problem in the impact limit has been treated by Ben-Reuven[23] and by Pasmanter and Ben-Reuven.[24] These authors point out that only cross correlations in the molecular excitation, where the excitation begins at one molecule and ends up at another, contribute to impact-regime linear density broadening and shifting due to resonance collisions. The matrix elements responsible for vibrational-to-vibrational (v-v) energy transfer processes that contribute to resonance-collision density shifts can be readily identified in semiclassical calculations of line shifting in hydrogen.[5,8–10,25] In these calculations, the intermolecular potential is expanded in a power series in the internuclear distance (the vibrational coordinate) of each molecule to account for vibrational dephasing and line shifting. The first term in this expansion that leads to resonant transfer of vibrational excitation is a second-order cross product proportional to each of the internuclear coordinates of the colliding molecules. In the early work on the coupling shift,[9,10] such a term in the expansion, based on the London formula, of the attractive (dispersion force) C_6 term in a Lennard-Jones potential was found to quantitatively predict the shift. Since the inclusion of similar terms in the expansion of the repulsive potential resulted in cancellations and too small of an effect, these authors assumed that the cross term (in the vibrational coordinates of the two molecules) in the repulsive part of the intermolecular potential was negligible.

The expansion of the C_6 term given by May *et al.*[9] was also applied by Bonamy *et al.*[25] to predict the overall shift in self-broadened HD (no evidence of a coupling shift has been seen for this system[26]). The potential employed by Bonamy *et al.* does include a cross term in a Lennard-Jones C_{12} repulsive core; however, since the overall shift in HD is strongly negative there is little evidence for this term in the repulsive potential. In fact, the Lennard-Jones R^{-12} repulsive potential has been found generally not to be appropriate for hydrogen and its isotopes (see Ref. 22).

The most extensive calculation of the vibrational shifts in H_2 is the semiclassical work of Kelley and Bragg.[5] These authors estimate the coefficients of the vibrational coordinate expansion of an attractive C_6, C_8, and C_{10} potential from an *ab initio* calculation of the H_2-He potential[27] and assume a similar expansion of the standard exponential repulsive core (see, for example, Ref. 22). Their form of the repulsive potential provides two parameters (the coefficients of the terms linear and quadratic in the vibrational coordinate of *one* of the molecules) which are adjusted to fit the measured shift coefficients. The overall temperature dependence of the shift, with the coupling shift removed, is accurately predicted by this calculation from 85 K through the highest-temperature (315 K) data used (see Fig. 6). Under the assumption, for both the attractive and repulsive parts of the potential, that the coefficient of the cross term is simply the square of the coefficient of the linear term (product function rule), the coupling shift is also predicted by these parameters. The values of these two parameters which provide the agree-

ment shown in Fig. 6, however, do not predict the magnitude or temperature dependence of the coupling shift. Kelley and Bragg observe that, while not physically justifiable within the context of their model, if they suppress the repulsive part of the cross terms they could predict the observed coupling shift. This observation is consistent with that of May *et al.*[9] in that the coupling shift can be predicted only if contributions by the repulsive part of the interaction potential are ignored.

The fact that we observe a trend to negative shifts with increasing population even at high temperature, where the average shift is strongly positive, serves to indicate further our poor understanding, in the context of current theory, of the role of the repulsive potential in the coupling shift. The connection between resonant-collision effects and v-v transfer[23,24] might lead us to look for insight from other experimental and theoretical studies involving v-v transfer. While an experimental (near-resonant) v-v transfer rate between the ortho- and parahydrogen species has been measured[28] and compared to calculations,[29] this process involves a finite energy gap that greatly reduces the contributions from long-range forces. Thus it is not surprising that these calculations[29] indicate a fairly strong temperature dependence and a weak contribution from long-range forces to the near-resonant v-v transfer rate. In contrast to this, if we accept the coupling-shift and resonance-collision argument, the near temperature independence of the resonance-shift coefficient, as well as its negative value, argue that long-range, attractive forces are dominant for exactly resonant v-v transfer. This would appear to hold even at high temperatures, where the overall shift is strongly dominated by the repulsive part of the interaction potential.

Resonance collisions should also be manifest in the J dependence of the vibrational-dephasing contribution to the linewidths. The important contribution of resonant v-v transfer to the widths of other molecular transitions has been discussed in the literature. (See, for example, Refs. 30 and 31.) Several authors[14,32,33] have commented on such a contribution in pure H_2. To our knowledge, such effects have not been identified explicitly in theoretical calculations. Thus there is still a considerable gap between experiment and theory in our understanding of the possible role of resonance collisions in H_2. It is hoped that, as H_2-H_2 interaction potentials are improved[34] and quantum scattering calculations become feasible,[35] it may be possible to gain additional insight into the vibrational dependence of the interaction potential and the role of resonance collisions in the H_2 self-density-shift and broadening coefficients.

CONCLUSIONS

The J and temperature dependence of the H_2 Raman Q-branch self-density-shift coefficients have been measured at high temperatures for the first time. The population-correlated J dependence of these coefficients, previously established at lower temperatures as a coupling shift, is observed to persist, almost independent of temperature, up to 1000 K. A new J dependence has also been found at high temperature and the overall temperature dependence is significantly different from extrapolations of current theoretical calculations. It is expected that these results, coupled with further theoretical efforts, will help elucidate the nature of the H_2-H_2 interaction potential, the role of resonance collisions, and the process of vibrational dephasing by collisions. These results have also allowed calculations of speed-dependent line-shift cross sections that have important implications for line-shape analysis of H_2 vibrational Raman spectra.[36]

ACKNOWLEDGMENTS

The authors would like to acknowledge useful discussions with R. L. Farrow, J. P. Looney, and J. D. Kelly, and expert technical assistance provided by Steve Gray in performing these experiments. This work was supported by the U.S. Department of Energy, Office of Basic Energy Sciences, Chemical Sciences Division, and by the U.S. Army Research Office.

[1]W. B. Roh, P. W. Schreiber, and J. P. E. Taran, Appl. Phys. Lett. **29**, 174 (1976). For a recent review of combustion applications see A. C. Eckbreth, *Laser Diagnostics for Combustion Temperature and Species* (Abacus, Cambridge, MA, 1988).

[2]M. Pealat, J. P. E. Taran, J. Taillet, M. Bacal, and A. M. Bruneteau, J. Appl. Phys. **52**, 2687 (1981).

[3]C. Schwartz and J. J. LeRoy, J. Mol. Spectrosc. **121**, 420 (1987).

[4]D. Robert, J. Bonamy, J. P. Sala, G. Levi, and F. Marsault-Herail, Chem. Phys. **99**, 303 (1985).

[5]J. D. Kelley and S. L. Bragg, Phys. Rev. A **34**, 3003 (1986).

[6]F. Rasetti, Phys. Rev. **85**, 937 (1929).

[7]B. P. Stoicheff, Can. J. Phys. **35**, 730 (1957).

[8]A. D. May, V. Degen, J. C. Stryland, and H. L. Welsh, Can. J. Phys. **39**, 1769 (1961).

[9]A. D. May, G. Varghese, J. C. Stryland, and H. L. Welsh, Can. J. Phys. **42**, 1058 (1964).

[10]E. C. Looi, J. C. Stryland, and H. L. Welsh, Can. J. Phys. **56**, 1102 (1978).

[11]P. Lallemand, P. Simova, and G. Bret, Phys. Rev. Lett. **17**, 1239 (1966).

[12]P. Lallemand and P. Simova, J. Mol. Spectrosc. **26**, 262 (1968).

[13]J. R. Murray and A. Javan, J. Mol. Spectrosc. **42**, 1 (1972).

[14]W. K. Bischel and J. Dyer, Phys. Rev. A **33**, 3113 (1986).

[15]N. E. Moulton, G. H. Watson, Jr., W. B. Daniels, and D. M. Brown, Phys. Rev. A **37**, 2475 (1988).

[16]D. E. Jennings, A. Weber, and J. W. Brault, J. Mol. Spectrosc. **126**, 19 (1987).

[17]J. O. Hirschfelder, C. F. Curtiss, and R. B. Bird, *Molecular Theory of Gases and Liquids* (Wiley, New York, 1964).

[18]L. A. Rahn, R. L. Farrow, M. L. Koszykowski, and P. L. Mattern, Phys. Rev. Lett. **45**, 620 (1980).

[19]R. L. Farrow and L. A. Rahn, in *Raman Spectroscopy: Linear and Nonlinear,* edited by J. Lascombe and P. V. Huong (Wiley, New York, 1982), p. 159.

[20]G. J. Rosasco, L. A. Rahn, W. S. Hurst, R. E. Palmer, J. P.

Looney, and J. W. Hahn, in *Pulsed Single-Frequency Lasers: Technology and Applications,* edited by W. K. Bischel and L. A. Rahn, (SPIE, Bellingham, 1988), Vol. 912, p. 171.
[21]A. E. DePristo, J. Chem. Phys. **74**, 36 (1987).
[22]J. Van Kranendonk, *Solid Hydrogen, Theory of the Properties of Solid H_2, HD, and D_2,* (Plenum, New York, 1983).
[23]A. Ben-Reuven, Phys. Rev. A **4**, 2115 (1971).
[24]R. A. Pasmanter and A. Ben-Reuven, J. Quant. Spectrosc. Radiat. Transfer **13**, 57 (1973).
[25]J. Bonamy, L. Bonamy, and D. Robert, J. Chem. Phys. **67**, 4441 (1977).
[26]G. J. Rosasco, A. D. May, W. S. Hurst, L. B. Petway, and K. C. Smyth, J. Chem. Phys. **90**, 2115 (1989).
[27]W. Meyer, P. C. Hariharan, and W. Kutzelnigg, J. Chem. Phys. **73**, 1880 (1980).
[28]R. L. Farrow and D. W. Chandler, J. Chem. Phys. **89**, 1994 (1988).
[29]G. D. Billing and E. R. Fisher, Chem. Phys. **18**, 225 (1976).
[30]See, for example, M. L. Strekalov and A. I. Burshtein, Chem. Phys. **82**, 11 (1983).
[31]A. V. Storozhev and M. L. Strekalov, Opt. Spektrosk. **64**, 1245 (1988) [Opt. Spectrosc. (USSR) **64**, 742 (1988)].
[32]E. J. Allin, A. D. May, B. P. Stoicheff, J. C. Stryland, and H. L. Welsh, Appl. Opt. **6**, 1597 (1967).
[33]C. G. Gray and H. L. Welsh, in *Essays in Structural Chemistry,* edited by A. J. Cowns, D. A. Long, and L. A. K. Staveley (Plenum, New York, 1971).
[34]W. K. Köhler and J. Schaefer, J. Chem. Phys. **78**, 4862 (1983).
[35]D. W. Schwenke and D. G. Truhlar, J. Chem. Phys. **88**, 4800 (1988).
[36]R. L. Farrow, L. A. Rahn, G. O. Sitz, and G. J. Rosasco, Phys. Rev. Lett. **63**, 746 (1989).